Mon. Not. R. Astron. Soc. **378,** 1461–1470 (2007) doi:10.1111/j.1365-2966.2007.11887.x

The white dwarf luminosity function – II. The effect of the measurement errors and other biases

Santiago Torres,[1,2] Enrique García-Berro[1,2⋆] and Jordi Isern[2,3]

[1]*Departament de Fí sica Aplicada, Escola Politècnica Superior de Castelldefels, Universitat Politècnica de Catalunya, Avda. del Canal Olí mpic s/n, 08860 Castelldefels, Spain*
[2]*Institut d'Estudis Espacials de Catalunya, c/Gran Capità 2–4, Edif. Nexus 104, 08034 Barcelona, Spain*
[3]*Institut de Ciències de l'Espai, CSIC, Campus UAB, Facultat de Ciències, Torre C-5, 08193 Bellaterra, Spain*

Accepted 2007 April 20. Received 2007 April 19; in original form 2007 January 28

ABSTRACT

The disc white dwarf luminosity function is an important tool for studying the solar neighbourhood, since it allows the determination of several Galactic parameters, the most important one being the age of the Galactic disc. However, only the $1/\mathcal{V}_{\rm max}$ method has been employed so far for observationally determining the white dwarf luminosity function, whereas for other kind of luminosity functions several other methods have been frequently used. Moreover, the procedures to determine the white dwarf luminosity function are not free of biases. These biases have two different origins: they can either be of statistical nature or a consequence of the measurement errors. In a previous paper we carried out an in-depth study of the first category of biases for several luminosity function estimators. In this paper we focus on the biases introduced by the measurement errors and on the effects of the degree of contamination of the input sample used to build the disc white dwarf luminosity function by different kinematical populations. To assess the extent of these biases we use a Monte Carlo simulator to generate a controlled synthetic population and analyse the behaviour of the disc white dwarf luminosity function for several assumptions about the magnitude of the measurement errors and for several degrees of contamination, comparing the performances of the most robust luminosity function estimators under such conditions.

Key words: methods: statistical – stars: luminosity function, mass function – white dwarfs – Galaxy: stellar content.

1 INTRODUCTION

White dwarf stars are well-studied objects from both the theoretical and observational point of view. Hence, the disc white dwarf luminosity function provides us with an invaluable wealth of information about the solar neighbourhood. Consequently, several important Galactic parameters can be derived from the observational white dwarf luminosity function. Among these parameters the most important ones are the age of the Galaxy (Winget et al. 1987; García-Berro et al. 1988; Hernanz et al. 1994; Richer et al. 2000) and the stellar formation rate (Noh & Scalo 1990; Díaz-Pinto et al. 1994; Isern et al. 1995; Isern, García-Berro & Salaris 2001). Additionally, the luminosity function of disc white dwarfs provides an independent test of the theory of dense plasmas (Segretain et al. 1994; Isern et al. 1997). Finally, the white dwarf luminosity function directly measures the current death rate of low- and intermediate-mass stars in the local disc, which also provides us with an important tool to evaluate stellar evolutionary sequences.

⋆E-mail: garcia@fa.upc.es

The advent of large automated surveys – like the Sloan Digital Sky Survey (SDSS; York et al. 2000; Stoughton et al. 2002; Abazajian et al. 2003, 2004; Eisenstein et al. 2006), the Two Micron All Sky Survey (Skrutskie et al. 1997; Cutri et al. 2003), the SuperCosmos Sky Survey (Hambly et al. 2001a,b; Hambly, Irwin & MacGillivray 2001c), the 2dF QSO Redshift Survey (Vennes et al. 2002), the SPY project (Pauli et al. 2003), and others – has dramatically increased the number of known white dwarfs. Future astrometric space missions – of which *Gaia* (Perryman et al. 2001) is the leading example – will undoubtedly increase even more the size of the white dwarf population with accurately determined parameters (Torres et al. 2005). However, this rapid increase in both the quality and the amount of observational data has not been accompanied by the corresponding developments in the way in which this wealth of observational data is analysed. Thus, there is a need to assess the reliability of the current methods used to estimate the disc white dwarf luminosity function – basically the $1/\mathcal{V}_{\rm max}$ method (Schmidt 1968) – and to test other techniques which allow more accurate determinations of the luminosity function. At this point it is worth mentioning that new luminosity function estimators have been specifically devised to solve several long-standing problems for the case in which galaxy

luminosity functions have to be obtained. For instance, the C^- method (Lynden-Bell 1971), the STY method (Sandage, Tammann & Yahil 1979), the Choloniewski method (Choloniewski 1986) and the Stepwise Maximum Likelihood method (Efstathiou, Ellis & Peterson 1988), among other methods, are currently used to derive galaxy luminosity functions. Bivariate luminosity functions derived from the mixture of two or more populations, non-homogeneity biases and the effects of anisotropies or clustering, are some examples of the kind of problems that must be faced nowadays and that these improved estimators are expected to correctly address.

Very few works have studied the reliability of the $1/\mathcal{V}_{\rm max}$ method when applied to the case of the white dwarf luminosity function. The two preliminary studies of Wood & Oswalt (1998) and García-Berro et al. (1999) demonstrated – using two independent Monte Carlo simulators – that the $1/\mathcal{V}_{\rm max}$ method for proper motion selected samples is a good density estimator, although it shows important statistical fluctuations when estimating the slope of the bright end of the white dwarf luminosity function. In the latter of these works it was also shown that a bias in the derived ages of the solar neighbourhood is present, consequence of the binning procedure. Additionally, it has been recently shown (Geijo et al. 2006) that the size of the observational error bars assigned by the $1/\mathcal{V}_{\rm max}$ method is severely underestimated and that more robust luminosity function estimators can be used. These estimators provide a good characterization of the shape of the white dwarf luminosity function even in the case in which a small number of objects is used. Even more, in this last study it was found that for a small sample size the $1/\mathcal{V}_{\rm max}$ method provides a poor characterization of the less populated bins, while for large samples the performances of the Choloniewski method and of the $1/\mathcal{V}_{\rm max}$ method are very similar, providing with a reasonable accuracy both the shape of the disc white dwarf luminosity function and the precise location of the cut-off. Finally, the main conclusion obtained in this study was that in order to obtain a reliable observational white dwarf luminosity function both estimators, the $1/\mathcal{V}_{\rm max}$ method and the Choloniewski method, can be used, while other parametric maximum likelihood estimators are not recommended.

However, the approach adopted in Geijo et al. (2006) focused only on the statistical techniques used to obtain the disc white dwarf luminosity function, whereas the effects of the observational errors and the contamination by different kinematical population were totally disregarded. The present paper aims precisely at filling in this gap. Specifically, we study the Lutz–Kelker bias – see below for a description of this bias – and the effects of the contamination by different kinematical populations of the input sample used to build the disc white dwarf luminosity function. To do this we use a Monte Carlo simulator to generate a controlled synthetic population and analyse the behaviour of the disc white dwarf luminosity function for several assumptions about the magnitude of the measurement errors and for several degrees of contamination, comparing the performances of the most robust luminosity function estimators under such conditions.

The paper is organized as follows. In Section 2, we briefly remind the reader the basics of the different estimators that can be used to derive the white dwarf luminosity function, and we argue which are best fitted for our purpose. In Section 3 we outline the main ingredients of the Monte Carlo simulations used to generate a synthetic population of white dwarfs to which we apply the previously described estimators. A systematic study of the effects on the white dwarf luminosity function of the measurement errors and of the contamination by different kinematical populations is performed in Section 4. Finally, in Section 5, we summarize our major findings and we draw our conclusions.

2 THE LUMINOSITY FUNCTION ESTIMATORS

The $1/\mathcal{V}_{\rm max}$ has been the only method used up to now for observationally determining the disc white dwarf luminosity function. Since its introduction by Schmidt (1968) in the studies of the quasar population, it has been extended to proper motion selected samples (Schmidt 1975) and generalized in order to introduce the dependence on the direction of the sample (Felten 1976). This turns out to be useful when studying stellar samples because the scaleheight of the Galactic disc introduces some biases. Basically, the $1/\mathcal{V}_{\rm max}$ method computes the maximum volume for which a star could be a member of the selected sample given a certain proper motion and magnitude limits. The contribution of each object to its magnitude bin is proportional to the inverse of its maximum volume and the luminosity function is built performing a weighted sum over the objects in each magnitude bin. Despite the fact that the $1/\mathcal{V}_{\rm max}$ method has been extensively used in different instances – it has been used not only to derive the luminosity function of the disc white dwarf population but also to obtain luminosity functions of main-sequence stars and quasars – and provides a reasonable estimate of the real luminosity function with an easy computational implementation it also has important drawbacks. The most important one is that it has been shown that the $1/\mathcal{V}_{\rm max}$ method should only be used when both the homogeneity and the completeness of the sample under study are guaranteed. This, obviously, is not an easy task and for most of the observational samples it is an 'a priori' assumption. Nevertheless, for the case of the white dwarf luminosity function this is the technique usually adopted for observationally determining the disc white dwarf luminosity function.

There exist other alternatives to the $1/\mathcal{V}_{\rm max}$ method, mostly based on a maximum likelihood analysis of the data. Among them, the Choloniewski method (Choloniewski 1986) is probably one of the most widely used methods. The basic premise of this method is that the local distribution of objects in some pair of variables of the sample has a Poissonian distribution. Then, it is possible to define a likelihood as a function of the parameter space. The Choloniewski method divides the parameter space (magnitude and parallax in our case) in cells and assumes Poissonian statistics for each cell – see, for instance, Geijo et al. (2006), and references therein, for a complete description of this method. Other maximum likelihood estimators can be used, but for the case of the disc white dwarf luminosity function the Choloniewski method turns out to be the most appropriate one, as shown in Geijo et al. (2006). This is the reason why in this paper we will only compare the performances of these two methods.

3 THE MONTE CARLO SIMULATIONS

Since we want to study the behaviour of the estimators previously discussed in Section 2 for the realistic case in which two different kinematical populations are present, we have built synthetic white dwarf populations in which both disc and halo white dwarfs are generated using Monte Carlo techniques. We have thoroughly described our Monte Carlo simulator in previous papers (García-Berro et al. 1999; Torres et al. 2002; García-Berro et al. 2004) so here we will only summarize the most important inputs.

We have used a pseudo-random number generator algorithm (James 1990) which provides a uniform probability density within the interval (0, 1) and ensures a repetition period of $\gtrsim 10^{18}$, which is virtually infinite for practical purposes. When Gaussian probability functions are needed, we have used the Box–Muller algorithm (Press

et al. 1986). Each one of the Monte Carlo simulations discussed in Section 4 consists of an ensemble of 40 independent realizations of the synthetic white dwarf population, for which the average of any observational quantity along with its corresponding s.d. was computed. Here the s.d. means the ensemble mean of the sample dispersions for a typical sample.

We start with the disc model. First, masses and birth times are drawn according to a standard initial mass function (Scalo 1998) and an exponentially decreasing star formation rate per unit surface area (Bravo, Isern & Canal 1993; Isern et al. 1995). The spatial density distribution is obtained from a scaleheight law (Isern et al. 1995) which varies with time and is related to the velocity distributions – see below – and an exponentially decreasing surface density in the Galactocentric distance. The velocities of the simulated stars are drawn from Gaussian distributions. The Gaussian distributions take into account both the differential rotation of the disc and the peculiar velocity of the Sun (Dehnen & Binney 1997). The three components of the velocity dispersion ($\sigma_{\rm U}, \sigma_{\rm V}, \sigma_{\rm W}$) and the lag velocity V_0 are not independent of the scaleheight but, instead, are taken from the fit of Mihalas & Binney (1981) to main-sequence star counts. It is important to notice at this point that with this description we recover both the thick and the thin disc populations, and, moreover, we obtain an excellent fit to the disc white dwarf luminosity function (García-Berro et al. 1999). The adopted age of the disc is 11 Gyr. Finally, the disc simulations have been normalized to the local space density of disc white dwarfs within 250 pc, $n = 0.5 \times 10^{-3}$ pc^{-3} for $M_V < 12.75$ mag (Liebert, Bergeron & Holberg 2005).

For the halo population we adopt a typical isothermal, spherically symmetric halo with a density profile given by the expression

$$\rho(r) = \rho_0 \frac{a^2 + {\rm R}_\odot^2}{a^2 + r^2}, \tag{1}$$

where $a \approx 5$ kpc is the core radius, ρ_0 is the local halo density and ${\rm R}_\odot = 8.5$ kpc is the Galactocentric distance of the Sun. The velocity distributions are Gaussian:

$$f(v_r, v_\theta, v_\phi) = \frac{1}{(2\pi)^{3/2}} \frac{1}{\sigma_r \sigma_t^2} \exp\left[-\frac{1}{2}\left(\frac{v_r^2}{\sigma_r^2} + \frac{v_\theta^2 + v_\phi^2}{\sigma_t^2}\right)\right]. \tag{2}$$

The radial and tangential velocity dispersions are determined from Marković & Sommer-Larsen (1997). For the radial velocity dispersion we have

$$\sigma_r^2 = \sigma_0^2 + \sigma_+^2 \left[\frac{1}{2} - \frac{1}{\pi} \arctan\left(\frac{r - r_0}{l}\right)\right], \tag{3}$$

where $\sigma_0 = 80$ km s^{-1}, $\sigma_+ = 145$ km s^{-1}, $r_0 = 10.5$ kpc and $l = 5.5$ kpc. The tangential dispersion is given by

$$\sigma_t^2 = \frac{1}{2} V_{\rm c}^2 - \left(\frac{\gamma}{2} - 1\right)\sigma_r^2 + \frac{r}{2}\frac{{\rm d}\sigma_r^2}{{\rm d}r}, \tag{4}$$

where

$$r\frac{{\rm d}\sigma_r^2}{{\rm d}r} = -\frac{1}{\pi}\frac{r}{l}\frac{\sigma_+^2}{1 + [(r - r_0)/l]^2}. \tag{5}$$

For the calculations reported here we have adopted a circular velocity $V_{\rm c} = 220$ km s^{-1}. The halo was assumed to be formed in an intense burst of star formation that occurred 14 Gyr ago and lasted for 1 Gyr.

For both sets of Monte Carlo simulations the initial-to-final mass relationship is that of Iben & Laughlin (1989). The main-sequence lifetimes of the progenitors of white dwarfs is also taken from Iben & Laughlin (1989). Finally, the cooling sequences of Salaris et al. (2000) have been used. These cooling sequences incorporate the most accurate physical inputs for the stellar interior (including neutrinos, crystallization and phase separation) and reproduce the blue turn at low luminosities (Hansen 1998). Also, these cooling sequences encompass the range of interest of white dwarf masses, therefore a complete coverage of the effects of the mass spectrum of the white dwarf population was taken into account.

4 RESULTS

4.1 A sample with known parallaxes

We have first simulated a disc white dwarf sample with known parallaxes. For a realistic observational sample this is equivalent to saying that the maximum distance for which a white dwarf can enter into the sample is ∼250 pc. This is the case, for instance, of the catalogue of spectroscopically identified white dwarfs of McCook & Sion (1999), where the minimum parallax is ≈0.003 arcsec. In order to build the final sample from which the white dwarf luminosity function is obtained, we have chosen the following criteria: $m_V \leqslant 18.5$ mag and $\mu \geqslant 0.16$ arcsec yr^{-1} as it was done in Oswalt et al. (1996). Additionally, all white dwarfs brighter than $M_V \leqslant 13$ mag are included in the sample, regardless of their proper motions, since the luminosity function of hot white dwarfs has been obtained from a catalogue of spectroscopically identified white dwarfs (Green 1980; Fleming, Liebert & Green 1986) which is assumed to be complete (Liebert, Bergeron & Holberg 2005). Moreover, all white dwarfs with tangential velocities larger than 250 km s^{-1} were discarded (Liebert, Dahn & Monet 1989) since these would be probably classified as halo members, according to the most widely used procedure. Finally, we have added random measurement errors to the proper motions, apparent magnitudes and parallaxes of all white dwarfs. The measurement errors were drawn from Gaussian distributions with the following deviations: $\sigma_\mu = 4$ mas yr^{-1}, $\sigma_{m_V} = 0.02 m_V$ and $\sigma_\pi = 0.167\pi$, which are realistic values (Luri et al. 1996; Harris et al. 2006).

In Fig. 1 we show the disc white dwarf luminosity functions obtained using this method, for both the case in which the measurement errors were disregarded (open symbols) and the case in which the measurement errors were fully taken into account (filled symbols). The open symbols have been shifted by $\Delta\log(L/{\rm L}_\odot) = -0.08$ for the sake of clarity. In the upper panel the results obtained using the $1/\mathcal{V}_{\rm max}$ method are shown whereas in the bottom panel we display the results obtained using the Choloniewski estimator. We recall that, by construction, our samples are complete, although we only select about 300 white dwarfs using the selection criteria discussed before. However, our simulations do provide the whole population of white dwarfs, which is much larger. Hence, we can obtain the *real* luminosity function by simply counting white dwarfs in the computational volume. This is done for all realizations and thereafter we obtain the average. The result is depicted as a solid line in Fig. 1. The true luminosity function steadily increases for luminosities larger than $\log(L/{\rm L}_\odot) \simeq -4.7$ and then it decreases. The sharp drop at $\log(L/{\rm L}_\odot) \simeq -4.9$ is an artefact of the numerical procedure because no white dwarfs more massive than $M_{\rm WD} \simeq 1.1\,{\rm M}_\odot$ have been simulated. The reason for this is that no reliable cooling sequences were available until very recent times (Althaus et al. 2007).

We focus first on the overall shape of the luminosity function and later we study the position of the cut-off. Both estimators recover with a relatively good degree of accuracy the slope of the increasing branch of the disc white dwarf luminosity function. However, the

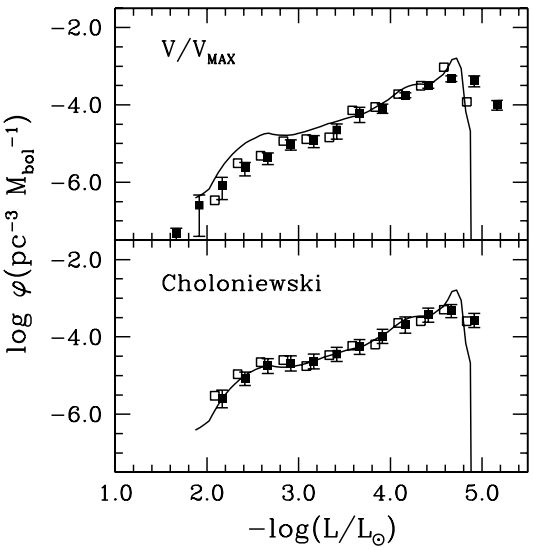

Figure 1. White dwarf luminosity function for a simulated sample in which the white dwarfs have known parallaxes for the cases in which no measurement errors are considered (open symbols) and adding proper motion, magnitude and parallax errors (solid symbols). The open symbols have been shifted by $\Delta\log(L/\mathrm{L}_\odot) = -0.08$ for the sake of clarity. The solid line shows the real luminosity function.

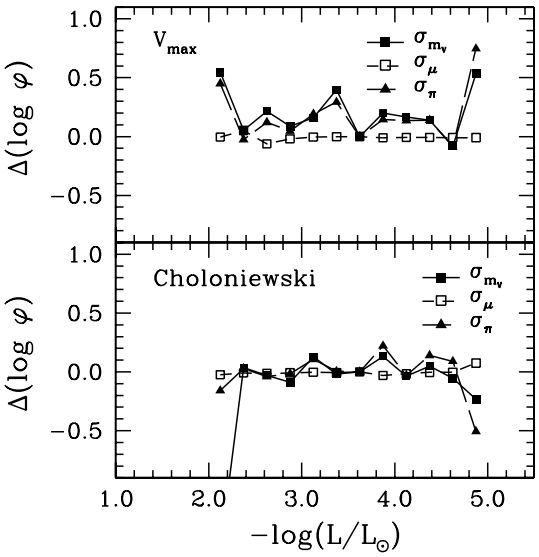

Figure 2. Differences of the resulting white dwarf luminosity function, $\Delta\log\phi$, when apparent magnitude (solid squares), proper motion (open squares) and parallax errors (solid triangles) are assumed, with respect to the white dwarf luminosity function with no errors added. See text for details.

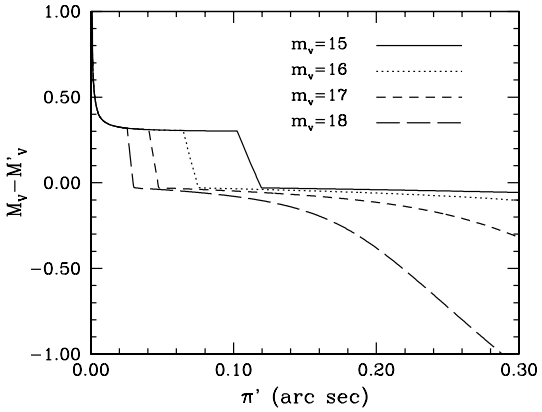

Figure 3. Differences between the true absolute magnitude, M, and the magnitude inferred from the raw parallax, M', as a function of the measured parallax π' for different apparent magnitudes m.

Choloniewski method performs much better than the $1/\mathcal{V}_{\max}$ estimator for luminosities larger than $\log(L/\mathrm{L}_\odot) = -3$. Specifically, the $1/\mathcal{V}_{\max}$ method shows a marked tendency to underestimate the density of white dwarfs for the brightest luminosity bins. This was already found in Geijo et al. (2006), and it is a bias which can be attributed to the limited distance of the sample. To be precise, for a magnitude-limited sample, bright white dwarfs can enter into the sample even if they are located at larger distances than faint stars. Although the $1/\mathcal{V}_{\max}$ method has been devised to remove this effect, the bias persists for bins with a small number of objects. Note that for both luminosity estimators, the effects of the measurement errors are small and, in most of the cases, the luminosity function in which the measurement errors were disregarded falls inside the 1σ error bars of the case in which we have added the measurement errors.

We now pay attention to the position of the cut-off of the disc white dwarf luminosity function. Both estimators recover fairly well the position of the cut-off of the white dwarf luminosity function for the case in which the measurement errors are not taken into account. However, the situation turns out to be different when the measurement errors are taken into account. As seen in the bottom panel of Fig. 1 the Choloniewski method also recovers very well the position of the cut-off in this case while the $1/\mathcal{V}_{\max}$ method does not, as clearly shown in the upper panel of Fig. 1. In particular, for this case the bins around the maximum appear to have smaller number densities and the cut-off of the white dwarf luminosity function is shifted to considerably smaller luminosities. Specifically, the position of the cut-off is shifted by $\Delta\log(L/\mathrm{L}_\odot) \simeq -0.3$. This bias in the determination of the cut-off has dramatic consequences, since the determination of the age of the solar neighbourhood relies on a precise determination of the position of the cut-off, and depending on the adopted cooling sequences and main-sequence lifetimes this systematic effect could amount to about 2 Gyr (García-Berro et al. 1999).

We now ask ourselves which is the respective contribution of each of the measurement errors to this behaviour. To state this in another way: which measurement errors are responsible for this shift to smaller luminosities of the position of the cut-off of the white dwarf luminosity function? To answer this question we have performed a series of calculations where the measurement errors have been added separately. The results are shown in Fig. 2. For the sake of clarity we have represented the logarithmic difference, $\Delta\log\varphi = \log\varphi' - \log\varphi$ of the luminosity function in which the measurement errors were taken into account, $\log\varphi'$, with respect to the white dwarf luminosity function in which no measurement errors were considered, $\log\varphi$. A first inspection of Fig. 2 reveals that the effects of introducing errors in proper motion are totally negligible whereas, as it could be expected, the effects of the parallax and apparent magnitude errors are dominant and tightly correlated. Additionally, these effects are more important for both the brightest and faintest luminosity bins, whereas the intermediate luminosity bins are not so largely affected. While both estimators are affected by the measurement errors, the $1/\mathcal{V}_{\max}$ method shows a stronger dependence on these for the faintest luminosity bins when compared

to the Choloniewski estimator. This behaviour corresponds to the expectations, given that the Choloniewski estimator is a maximum likelihood estimator and, consequently, the effects of a single object are thus smaller. Also remarkable is the fact that the effects of the measurement errors are of opposite sign. Generally speaking, it has been shown previously that when no measurement errors are taken into account, the tendency of the $1/\mathcal{V}_{\rm max}$ method is to underestimate the number density of white dwarfs in the less populated luminosity bins, whereas for the Choloniewski estimator the tendency is the opposite. However, when the measurement errors are incorporated the $1/\mathcal{V}_{\rm max}$ method shows a less marked tendency to underestimate the luminosity function in these bins and the Choloniewski method also produces a result which is closer to the real one.

4.2 The Lutz–Kelker bias

The error in the determination of the parallax for a small parallax-limited sample implies another kind of bias. First studied by Lutz & Kelker (1973), these authors showed that if we assume a monotonically decreasing distribution of true parallaxes, the errors would therefore scatter more stars into the sample (with positive errors) than out of it (with negative errors). Even more, this bias was demonstrated to be independent of the lower parallax limit and also of the parallax distribution. The main consequence of the Lutz–Kelker bias for a monotonically decreasing distribution of parallaxes is that the observed parallax results, on average, larger than its true value. Consequently, this overestimate of the parallax translates into an underestimate of the distance and, hence, into an underestimate of the luminosity of a given star. A complete discussion of the Lutz–Kelker bias can be found in Smith (2003). However, for our analysis we have closely followed the nomenclature of Binney & Merrifield (1998). Our main goal is to quantify the seriousness of the Lutz–Kelker bias for the white dwarf luminosity function and how do the two estimators under study perform for this particular case. We have proceeded as follows. We need to evaluate the probability $P(\pi|\pi')\,{\rm d}\pi$ that the true parallax of a given star, π, lies within (π, $\pi + {\rm d}\pi$) given that its measured parallax is π'. To do this we apply Bayes theorem:

$$P(\pi|\pi') = \frac{P(\pi'|\pi)P(\pi)}{P(\pi')}. \tag{6}$$

We do not need to evaluate the prior probability of the denominator, since it only appears as a normalization factor, but the numerator is of fundamental importance. Following Binney & Merrifield (1998), and after some elementary algebra, the next expression is obtained:

$$P(\pi|\pi') \propto P(\pi'|\pi)\Phi(M)\nu(s)\pi^{-4}, \tag{7}$$

where $P(\pi'|\pi){\rm d}\pi'$ is the probability that the observational errors will cause the parallax of a star, which has true parallax π, to be measured as π', $\Phi(M)$ is the absolute magnitude luminosity function and $\nu(s)$ is the space density of stars with $s = \pi^{-1}$. In order to evaluate the Lutz–Kelker bias we must make some assumptions with respect to the previous functions. First of all, we assume that the probability of measuring a parallax π' for an object whose true parallax is π is given by a Gaussian distribution with an s.d., σ_π, of the measurement errors. For the space density distribution and since parallaxes can only be measured for nearby stars, it is reasonable to assume that the distribution ν is independent of s. Finally, regarding the luminosity function $\Phi(M)$ we can take advantage of our synthetic population since we know the *true* shape of the luminosity function. We must remark here that this would not be the case of a real situation, where the luminosity function is not known 'a priori'. However, this problem can be solved in a practical situation by using an iterative procedure. Additionally, and for the case of the white dwarf luminosity function, the bright portion of the white dwarf luminosity function turns out to be rather insensitive to the star formation rate, which also eases the calculation of the luminosity function. Under these assumptions equation (7) can be written in the following way:

$$P(\pi|\pi') \propto \Phi(M)\pi^{-4}\exp\left[-\frac{(\pi'-\pi)^2}{2\sigma_\pi^2}\right], \tag{8}$$

where $M = m + 5\,\log\,(\pi/10)$. For any given measured apparent magnitude, m, and parallax, π', the value of π that maximizes the previous expression can be found. It is reasonable to take this value as the true value of the parallax and then estimate the true absolute magnitude, $M = M' + 5\,\log\,(\pi/\pi')$. In Fig. 3 we show the results obtained with this procedure for several apparent magnitudes, ranging from 15 to 18, as a function of the measured parallax. As seen in this figure, for small parallaxes the Lutz–Kelker bias implies an underestimate of the absolute magnitude, which could be as large as 1 mag. On the contrary, the effect for large parallaxes is the opposite. The magnitude can be largely overestimated for faint white dwarfs. It is worth noticing here that this estimate of the true absolute magnitude is independent of the luminosity function estimator and only depends on the assumptions adopted for evaluating equation (8) and, in particular, on the adopted luminosity function.

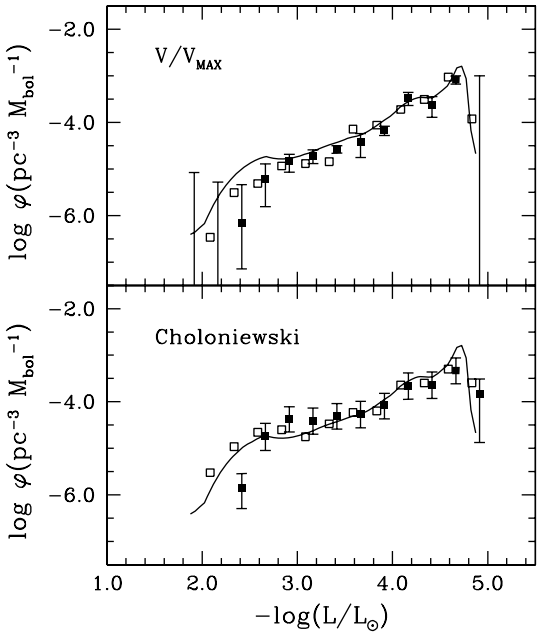

Figure 4. White dwarf luminosity function for a simulated sample with known parallaxes assuming no measurement errors (open symbols) and for the case in which measurement errors were taken into account but after correcting for the Lutz–Kelker bias (solid symbols).

Finally, in Fig. 4 we show the resulting white dwarf luminosity functions derived using either the $1/\mathcal{V}_{\rm max}$ method (top panel) or the Choloniewski estimator (bottom panel) after correcting for the Lutz–Kelker bias (solid symbols). As before, our real luminosity function is represented as a solid line and the luminosity function in which no measurement errors were incorporated is shown for the sake of comparison as open symbols. This figure shows that the effects of the Lutz–Kelker bias can be easily taken into account

and that once this is done we recover the correct position of the cut-off. For the rest of the bins the effects are not noticeable, as one should expect. Note as well that the size of the assigned error bars is considerably larger when compared to those obtained previously for both the luminosity bins of the brightest portion of the white dwarf luminosity function and for the bins at its faint end.

4.3 The SDSS simulation

The very recent publication of the SDSS Data Release 3 has notably increased the number of known white dwarfs and has also largely extended the search volume (Eisenstein et al. 2006). Moreover, the SDSS sample, combined with improved proper motions from the USNO-B has allowed to derive a preliminary (although very much improved) white dwarf luminosity function based on approximately 6000 stars (Harris et al. 2006). Both facts make this sample an ideal test bed for the kind of techniques we are dealing with. However, we recall here that the SDSS does not provide a parallax measurement and, hence, the distances are determined using the SDSS photometry. In particular, the distance is obtained using a colour–magnitude relationship for an otherwise typical $0.6\,\mathrm{M}_{\odot}$ white dwarf. Taking this into account, we have simulated a disc white dwarf population centred around the North Galactic Cap, up to a distance of 1800 pc and according to the precise geometry of the SDSS. For this simulation we have used a new set of selection criteria, which meet the characteristics of the SDSS (Harris et al. 2006). These selection criteria are the following: $15.0 < m_V < 19.5$ mag, $\mu > 20$ mas yr^{-1} and $V_{\tan} > 30\,\mathrm{km\,s^{-1}}$. Harris et al. (2006) also used the reduced proper motion $H_g = g + 5\log\mu + 5$, where g is the SDSS magnitude, to discriminate between main-sequence stars and white dwarfs, since the latter are typically 5–7 mag less luminous than subdwarfs of the same colour, and this is what we also do. As previously done, we have added the corresponding measurement errors. However, in this case, and given that the parallax is not directly measured we have only added proper motion and magnitude errors. The distributions of errors are again assumed to be Gaussian, and the corresponding s.d. values are $\sigma_\mu = 4$ mas yr^{-1} in proper motion, and $\sigma_{m_V} = 0.02\,m_V$ in apparent magnitude. The final size of the sample is roughly $\sim$2000 white dwarfs, which is very similar to the number of white dwarfs used by Harris et al. (2006).

The resulting white dwarf luminosity functions for the SDSS model simulation assuming no measurement errors (open symbols) and adding proper motion and magnitude errors (solid symbols) are shown in Fig. 5. We have represented once again the true luminosity function as a solid line. As seen, both estimators recover quite well both the shape of the increasing branch of the luminosity function and the position of the cut-off when no measurement errors are added. For the case of the $1/\mathcal{V}_{\max}$ method, the bias already mentioned for a distance-limited sample, consisting in underestimating the density of bright objects, is somewhat reduced, whereas the Choloniewski method slightly overestimates the star density for these luminosity bins. However, both methods yield satisfactory results, and we remark that these are minor effects. However, when the measurement errors are introduced, the position of the cut-off for the $1/\mathcal{V}_{\max}$ estimator is again shifted to smaller luminosities, whereas the Choloniewski method correctly retrieves the real cut-off. The reasons are identical to those previously discussed for the distance-limited sample – the Lutz–Kelker bias – and, thus, the Choloniewski method, which is less sensitive to this bias, turns out to be more robust when analysing this sample.

For the sake of completeness we have also evaluated how the measurement errors in magnitude and proper motion separately affect the white dwarf luminosity function. The results, presented as the logarithmic difference of the luminosity function, are shown in Fig. 6. The behaviour of both estimators is quite similar to those presented if Fig. 2. As seen, the error in apparent magnitude is the dominant source of errors for the faintest luminosity bins when the $1/\mathcal{V}_{\max}$ estimator is used, whereas the errors in proper motion play a very limited role – as it should be expected. This is also the case when the Choloniewski method is used but, for the case of the lowest luminosity bins, the effects are in any case smaller than when the $1/\mathcal{V}_{\max}$ method is employed.

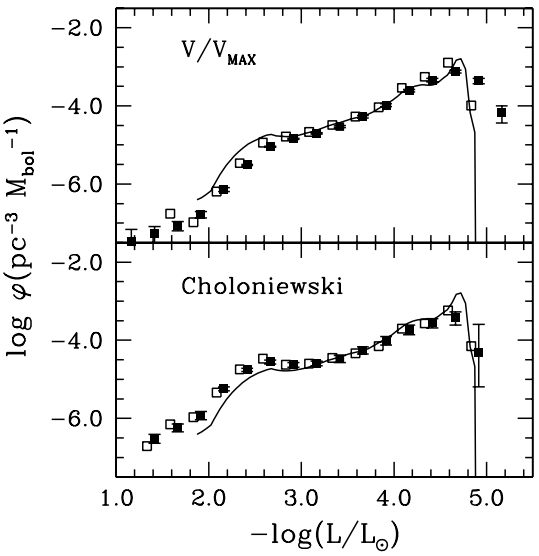

Figure 5. White dwarf luminosity functions for the SDSS model simulation assuming no measurement errors (open symbols) and adding proper motion and magnitude errors (solid symbols). The solid line represents the *real* luminosity function.

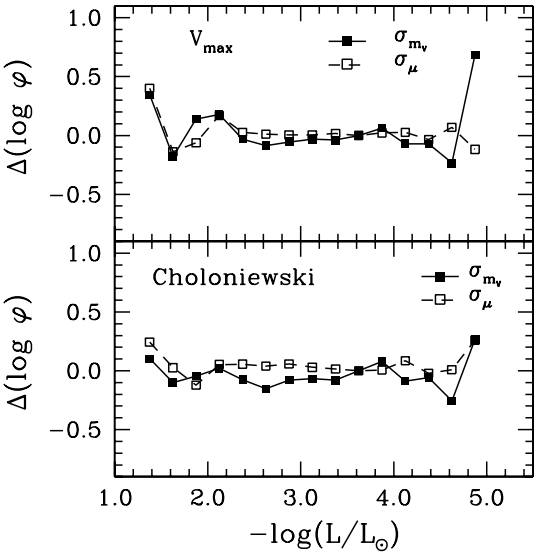

Figure 6. Differences of the resulting white dwarf luminosity function, $\Delta\log\phi$, when apparent magnitude (solid squares) and proper motion (open squares) are assumed, with respect to the white dwarf luminosity function with no errors added. See text for details.

4.4 Contamination by halo white dwarfs

Up to now we have been dealing with model white dwarf luminosity functions derived from synthetic populations which were derived from pure kinematical populations and, more particularly, from a sample of disc white dwarfs. However, there is some evidence that the faint end of the white dwarf luminosity function contains multiple kinematic populations, not only thin disc, but also thick disc and halo as well (Reid 2004). Although our model for the disc white dwarf population naturally incorporates the thick disc population, a careful evaluation of the effects of the contamination by the halo population still remains to be done. If, as expected, the sample from which the disc white dwarf luminosity function is built is contaminated by a small number of missclasified halo white dwarfs, this may have consequences on the location of the observed cut-off. However, this still remains to be assessed. In order to clarify the extent of such a possible bias and to assess which is the response of the different estimators to this bias, we have performed a series of simulations where we have introduced a certain degree of halo contamination. Since the SDSS has provided us with a large number of new white dwarfs it is more likely that a small degree of halo contamination should be present and, thus, we assess its effects using this last simulation. Additionally, and in order to see the real effects of a small admixture of halo white dwarfs in the resulting population, independently of the role played by the measurement errors, we use the simulation in which these measurement errors have been disregarded.

We proceed as follows. We simulate a population of halo white dwarfs within a total radius of 1800 pc. Then, we normalize the total number of halo white dwarfs using the halo white dwarf luminosity function of Torres, García-Berro & Isern (1998). That is, we impose that the density of halo white dwarfs in the local neighbourhood (250 pc) is $n \sim 1.2 \times 10^{-5}$ pc^{-3} for $\log\,(L/\mathrm{L}_{\odot}) \gtrsim -3.5$ (Torres et al. 1998). We then extract all halo white dwarfs which are in the direction of the region surveyed by the SDSS. After this we randomly include the selected synthetic halo white dwarfs in the disc sample. This results in total contamination of about 1 per cent. Although the total contamination turns out to be small, not all luminosity bins are equally affected, as seen in Fig. 7. In particular, the contamination of the brightest luminosity bins is moderate, but for the faintest luminosity bin the contamination of the disc sample with halo white dwarfs can be as large as 50 per cent – as it should be expected given that we have assumed that the halo star formation history was a burst of very short duration which occurred 14 Gyr ago (see below). Additionally, and since the local density of halo white dwarfs is still the subject of a strong debate, we have also adopted a much larger total density of halo white dwarfs of $n \sim 2.2 \times 10^{-4}$ pc^{-3}, as suggested by Oppenheimer et al. (2001). We stress that this value of the density of halo white dwarfs should be considered as an extreme upper limit. This results in a total contamination of the disc sample with halo white dwarfs of $\sim$10 per cent. However, as it was the case in which a modest contamination of the order of 1 per cent was discussed, not all luminosity bins are equally affected. In fact, in this case the effects are much more dramatic, as clearly seen in Fig. 7, and we find that the faintest luminosity bins of the white dwarf luminosity function are totally dominated by halo white dwarfs. Specifically, for the faintest luminosity bin we find that halo white dwarfs outnumber disc members by a factor of $\sim$3.5, whereas at luminosities of the order of $\log(L/\mathrm{L}_{\odot}) \simeq -4.0$, the degree of contamination can be as large as $\sim$20 per cent.

Now we ask ourselves which are the effects of such degrees of contamination in the resulting white dwarf luminosity function and how the different estimators perform in retrieving the correct luminosity function. To do this we repeat the procedure outlined in Section 4.3 to select the sample from which the white dwarf luminosity function is built, using the same selection criteria previously discussed: $15.0 < m_V < 19.5$ mag, $\mu > 20$ mas yr^{-1} and $V_{\tan} > 30$ km s^{-1}. The overall results are shown in the left-hand panels of Fig. 8. In this figure we have represented the uncontaminated disc white dwarf luminosity function (open symbols), the resulting

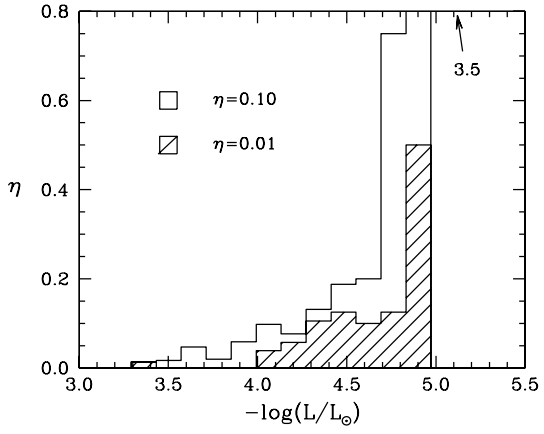

Figure 7. Contamination of the sample of disc white dwarfs with halo stars. The histograms show the fraction of halo white dwarfs with respect to the total number of stars for each luminosity bin as a function of the luminosity. The shaded histogram corresponds to a total contamination of the sample of 1 per cent, and the non-shaded histogram corresponds to a global contamination of 10 per cent. See text for details.

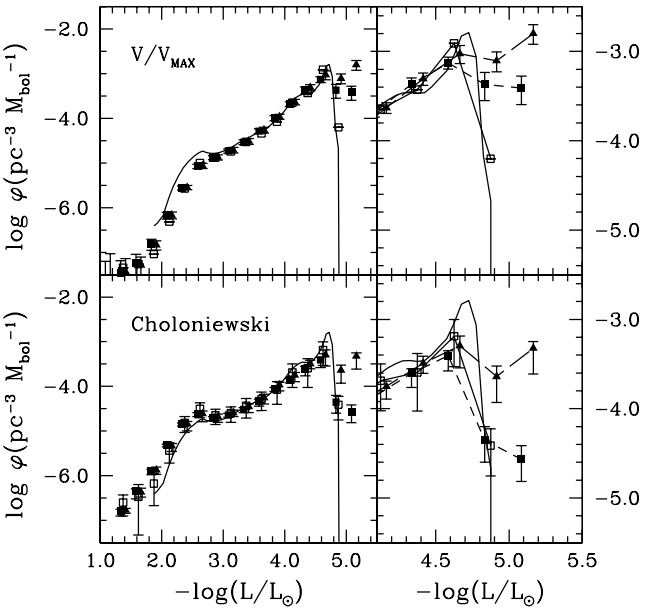

Figure 8. The white dwarf luminosity function for the SDSS simulation when a 1 per cent of halo contamination is assumed (solid squares) and assuming a 10 per cent of halo contamination (solid triangles). The uncontaminated white dwarf luminosity function is shown as open squares. The top panels show the results when the $1/\mathcal{V}_{\max}$ estimator is used, whereas the bottom panels depict the situation when the Choloniewski method is used. The right-hand panels show an enlarged view of the region of low luminosities. See text for details.

disc white dwarf luminosity function when a small admixture of 1 per cent of halo white dwarfs is added to the previous white dwarf population (solid squares), and the luminosity function obtained when an admixture of 10 per cent of halo white dwarfs is added to the uncontaminated disc white dwarf population (solid triangles). For the sake of clarity, the right-hand panels of Fig. 8 show an expanded view of the region of low luminosities. As previously done, the top panels represent the white dwarf luminosity functions obtained using the $1/\mathcal{V}_{\rm max}$ estimator, whereas the results obtained using the Choloniewski method are shown in the bottom panels.

As it should be expected from the previous discussion, the contamination by halo white dwarfs only affects the faintest bins of the disc white dwarf luminosity function. This is so because since all halo white dwarfs are almost coeval the halo white dwarf luminosity function is strongly peaked. However, for reasonable ages of the stellar halo, the peak of the halo white dwarf luminosity function is located at luminosities much smaller than that of the location of the cut-off of the disc white dwarf luminosity function. Consequently, the relative contribution of halo white dwarfs increases for decreasing luminosities. The different behaviours of both estimators are also quite apparent. As can be seen in the right-hand panels of Fig. 8, even a small degree of halo contamination – of the order of only $\sim$1 per cent, which corresponds to the halo white density derived by Torres et al. (1998) – strongly affects the shape of the disc white dwarf luminosity function for the case in which the $1/\mathcal{V}_{\rm max}$ estimator is used. In fact, the sharp drop-off in the number density of white dwarfs which characterizes the faint end of the white dwarf luminosity function is substituted by a shallow decrease when the degree of contamination is 1 per cent and a moderate increase when the degree of contamination is 10 per cent – which corresponds to the halo white dwarf density derived by Oppenheimer et al. (2001). However, the effects of the contamination by halo white dwarf are far less apparent when the Choloniewski estimator is used, as clearly shown in Fig. 8. If the Choloniewski method is used to derive the white dwarf luminosity function the correct position of the cut-off of the white dwarf luminosity function is still obtained when the degree of contamination is of 1 per cent, although an additional luminosity bin is obtained. On the contrary, when the contamination by halo white dwarfs is of the order of 10 per cent the drop-off of the disc white dwarf luminosity function is substituted by a shallow decrease and at even fainter luminosities the luminosity function increases, as it was the case when $1/\mathcal{V}_{\rm max}$ method was used. All in all, we find that the Choloniewski method turns out to be more robust against a possible contamination by halo white dwarfs.

Now, the question is can we reduce this bias? The most naïve and straightforward method to do this is to apply a velocity cut in order to separate the different kinematical populations. To test how effective is this widely spread technique for the case of the disc white dwarf luminosity function we adopt the most extreme case in which a 10 per cent contamination of the disc population by halo white dwarfs is assumed. The top panel of Fig. 9 shows the fraction of disc white dwarfs (solid line) and halo stars (dashed line) discarded using this procedure as a function of the velocity cut, $V_{\rm cut}$. Obviously, for large velocity cuts the fraction of disc stars discarded is totally negligible, and increases as the velocity cut decreases, as expected. The slope of the distribution turns out to be very steep for velocity cuts smaller than $\sim$120 km s^{-1}. Regarding the halo contamination it turns out that a velocity cut of $\sim$100 km s^{-1} discards $\sim$85 per cent of the contamination of the disc population by halo white dwarfs. The resulting white dwarf luminosity function is almost identical to that of the uncontaminated population. However, this velocity

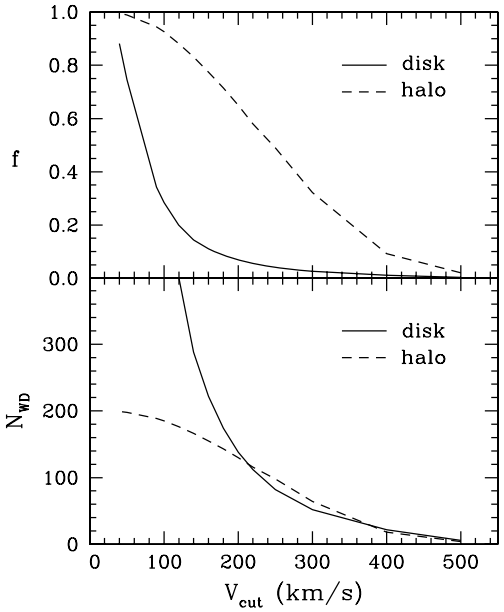

Figure 9. Top panel: fraction of white dwarfs discarded as a function of the velocity cut for both the disc and the halo populations. Bottom panel: total number of white dwarfs discarded for both populations as a function of the velocity cut.

cut can be somewhat relaxed. For instance, adopting a velocity cut of $\sim$250 km s^{-1} results in a disc white dwarf luminosity function totally equivalent to that already shown in Fig. 8 for the case in which a 1 per cent contamination was adopted. We recall that in this case the Choloniewski method gives a good result, whereas the $1/\mathcal{V}_{\rm max}$ estimator still gives a biased one. In this case the velocity cut must be reduced to $\sim$150 km s^{-1} in order to produce acceptable results. Thus, the necessary velocity cut to remove the halo contamination strongly depends on the adopted estimator, being considerably larger for the case in which the Choloniewski method is employed.

In principle, there is a wealth of information in the population of white dwarfs with large tangential velocities, that is, those which were discarded from the complete sample using the previously described procedure. Consequently, one may think that it should be feasible to build the halo white dwarf luminosity function using these stars. However, this is not the case. We illustrate the situation in the lower panel of Fig. 9. In this panel we show the total number of white dwarfs that are discarded using different velocity cuts for both the halo and the disc populations. These stars should be the natural candidates to enter into a pure halo sample. However, even for large velocity cuts the total numbers of disc and halo white dwarfs are very similar, thus preventing the derivation of a reliable halo white dwarf luminosity function. There are, however, more sophisticated ways of retrieving information from the high velocity tail. These methods are based in artificial intelligence techniques (Torres et al. 1998) and require the incorporation of more information about the target population like colours and magnitudes (among other characteristics) of the stars of the sample.

5 CONCLUSIONS

In this paper we have studied the biases introduced by the measurement errors on the disc white dwarf luminosity function. We have

done this for the case in which a small parallax-limited sample of about 300 white dwarfs is used and for a more interesting case in which a large sample of white dwarfs with photometrically derived distances is used. The first of these cases is representative of the current sample from which the disc white dwarf luminosity function is obtained, whereas the second case corresponds to the most recent sample of about 6000 white dwarfs obtained from the SDSS Data Release 3. We have also studied which luminosity function estimator is more robust, analysing the behaviour of the two luminosity function estimators that have been shown to perform best for the case of the disc white dwarf luminosity function when no measurement errors are taken into account, namely, the $1/\mathcal{V}_{\rm max}$ method and the Choloniewski method. For the case of a small parallax-limited sample we have found that the Lutz–Kelker bias is present and that it strongly affects the position of the cut-off of the white dwarf luminosity function when the $1/\mathcal{V}_{\rm max}$ estimator is used. This is not the case when the Choloniewski method is used. In this case, although the bias is present, the position of the cut-off remains almost unaffected. However, we have also shown that using the appropriate techniques this bias can be removed and the correct position of the cut-off of the disc white dwarf luminosity function can be retrieved, although at the price of considerably increasing the observational error bars. When a large sample of white dwarfs with photometric parallaxes is studied, the same behaviour is found. The $1/\mathcal{V}_{\rm max}$ method is found to be strongly biased, providing an erroneous location of the cut-off of the white dwarf luminosity function. This bias has important consequences since a precise determination of the age of the solar neighbourhood requires an accurate location of the drop-off. We have shown, however, that – as it was the case in which a small parallax-limited sample was used – the Choloniewski method turns out to be rather insensitive to the measurement errors and retrieves with rather good accuracy the position of cut-off of the white dwarf luminosity function.

Finally, we have also studied the response of both estimators to a potential contamination of the sample of the disc white dwarf population with halo white dwarfs. We have found that the effects of such contamination are quite evident even in the case of a modest degree of contamination (of the order of 1 per cent) when the $1/\mathcal{V}_{\rm max}$ method is used. The most apparent effect consists in a much shallower drop-off in the case of a 1 per cent degree of contamination. If the contamination is higher the drop-off actually disappears. When the Choloniewski method is used the position of the drop-off is found to be much less affected when a 1 per cent degree of contamination is adopted, although a new luminosity bin at the faint end of the white dwarf luminosity function – exclusively due to halo white dwarfs – shows up. This bias can be removed by using a velocity cut to cull from the sample only white dwarfs with relatively small tangential velocities. The precise value of the velocity cut depends on the employed estimator. We have found that a velocity cut of $\sim$250 km s^{-1} works fine for the case in which the Choloniewski method is employed. For the case in which the $1/\mathcal{V}_{\rm max}$ is used this velocity cut turns out to be considerably smaller, of the order of $\sim$150 km s^{-1}. Consequently, more white dwarfs are withdrawn from the original sample and the statistical significance of the resulting disc white dwarf luminosity function turns out to be smaller in this case. All in all, we find that the Choloniewski method (Choloniewski 1986) is much more robust than the $1/\mathcal{V}_{\rm max}$ method against measurement errors and a possible contamination of the input sample by halo white dwarfs. Its practical implementation is not difficult and, moreover, we have shown that it retrieves an unbiased estimate of the position of the cut-off of white dwarf luminosity function, which by itself is an important reward.

ACKNOWLEDGMENTS

Part of this work was supported by the MEC grants AYA05-08013-C03-01 and -02, by the European Union FEDER funds and by the AGAUR.

REFERENCES

Abazajian K. et al., 2003, AJ, 126, 2081
Abazajian K. et al., 2004, AJ, 128, 502
Althaus L. G., García-Berro E., Isern J., Córsico A. H., Rohrmann R. D., 2007, A&A, 465, 249
Binney J., Merrifield M., 1998, Galactic Astronomy. Princeton Univ. Press, Princeton, NJ
Bravo E., Isern J., Canal R., 1993, A&A, 270, 288
Choloniewski J., 1986, MNRAS, 223, 1
Cutri R. et al., 2003, The 2MASS All-Sky Catalog of Point Sources. Univ. Massachusetts and IPAC/California Institute of Technology
Dehnen W., Binney J., 1997, MNRAS, 285, L5
Díaz-Pinto A., García-Berro E., Hernanz M., Isern J., Mochkovitch R., 1994, A&A, 282, 86
Efstathiou G., Ellis R. S., Peterson B. A., 1988, MNRAS, 232, 431
Eisenstein D. J. et al., 2006, ApJS, 167, 40
Felten J. E., 1976, ApJ, 207, 700
Fleming T. A., Liebert J., Green R. F., 1986, ApJ, 308, 176
García-Berro E., Hernanz M., Mochkovitch R., Isern J., 1988, A&A, 193, 141
García-Berro E., Torres S., Isern J., Burkert A., 1999, MNRAS, 302, 173
García-Berro E., Torres S., Isern J., Burkert A., 2004, A&A, 418, 53
Geijo E. M., Torres S., Isern J., García-Berro E., 2006, MNRAS, 369, 1654
Green R. F., 1980, ApJ, 238, 685
Hambly N. C. et al., 2001a, MNRAS, 326, 1279
Hambly N. C., Davenhall A. C., Irwin M. J., MacGillivray H. T., 2001b, MNRAS, 326, 1315
Hambly N. C., Irwin M. J., MacGillivray H. T., 2001c, MNRAS, 326, 1295
Hansen B. M. S., 1998, Nat, 394, 860
Harris H. C. et al., 2006, AJ, 131, 571
Hernanz M., García-Berro E., Isern J., Mochkovitch R., Segretain L., Chabrier G., 1994, ApJ, 434, 652
Iben I. Jr, Laughlin G., 1989, ApJ, 341, 312
Isern J., García-Berro E., Hernanz M., Mochkovitch R., Burkert A., 1995, in Koester D., Werner K., eds, White Dwarfs. Springer-Verlag, Heidelberg, p. 19
Isern J., Mochkovitch R., García-Berro E., Hernanz M., 1997, ApJ, 485, 308
Isern J., García-Berro E., Salaris M., 2001, in von Hippel T., Simpson C., Manset N., eds, ASP Conf. Ser. Vol. 245, Astrophysical Ages and Timescales. Astron. Soc. Pac., San Francisco, p. 328
James F., 1990, Comput. Phys. Commun., 60, 329
Liebert J., Dahn C. C., Monet D. G., 1989, in Wegner G., ed., White Dwarfs. Springer-Verlag, Berlin, p. 15
Liebert J., Bergeron P., Holberg J. B., 2005, ApJS, 156, 47
Luri X., Mennessier M. O., Torra J., Figueras F., 1996, A&AS, 117, 405
Lutz T. E., Kelker D. H., 1973, PASP, 85, 573
Lynden-Bell D., 1971, MNRAS, 155, 95
Marković D., Sommer-Larsen J., 1997, MNRAS, 288, 733
McCook G. P., Sion E. M., 1999, ApJS, 121, 1
Mestel L., 1952, MNRAS, 112, 583
Mihalas D., Binney J., 1981, Galactic Astronomy. Freeman & Co., San Francisco
Noh H. R., Scalo J., 1990, ApJ, 352, 605
Oppenheimer B. R., Hambly N. C., Digby A. P., Hodgkin S. T., Saumon D., 2001, Sci, 292, 698
Oswalt T. D., Smith J. A., Wood M. A., Hintzen P., 1996, Nat, 382, 692
Pauli E. M., Napiwotzki R., Altmann M., Heber U., Odenkirchen M., Kerber F., 2003, A&A, 400, 877
Perryman M. A. C. et al., 2001, A&A, 369, 339

Press W. H., Flannery B. P., Teukolsky S. A., Vetterling W. T., 1986, Numerical Recipes, 2nd edn. Cambridge Univ. Press, Cambridge
Reid N., 2004, ARA&A, 43, 247
Richer H. B., Hansen B., Limongi M., Chieffi A., Straniero O., Fahlman G. G., 2000, ApJ, 529, 318
Salaris M., García-Berro E., Hernanz M., Isern J., Saumon D., 2000, ApJ, 544, 1036
Sandage A., Tammann G. A., Yahil A., 1979, ApJ, 232, 352
Scalo J., 1998, in Gilmore G., Howell D., eds, ASP Conf. Ser. Vol. 142, The Stellar Initial Mass Function. Astron. Soc. Pac., San Francisco, p. 201
Schmidt M., 1968, ApJ, 151, 393
Schmidt M., 1975, ApJ, 202, 22
Segretain L., Chabrier G., Hernanz M., García-Berro E., Isern J., Mochkovitch R., 1994, ApJ, 434, 641
Skrutskie M. F. et al., 1997, in Garzon F., Epchtein N., Omont A., Burton B., Perin P., eds, The Impact of Large Scale Near-IR Sky Surveys. Kluwer, Dordrecht, p. 25
Smith H. Jr, 2003, MNRAS, 338, 891
Stoughton C. et al., 2002, AJ, 123, 485
Torres S., García-Berro E., Isern J., 1998, ApJ, 508, L71
Torres S., García-Berro E., Burkert A., Isern J., 2002, MNRAS, 336, 971
Torres S., García-Berro E., Isern J., Figueras F., 2005, MNRAS, 360, 1381
Vennes S., Smith R. J., Boyle J., Croom S. M., Kawka A., Shanks T., Miller L., Loaring N., 2002, MNRAS, 335, 673
Winget D. E., Hansen C. J., Liebert J., van Horn H. M., Fontaine G., Nather R. E., Kepler S. O., Lamb D. Q., 1987, ApJ, 315, L77
Wood M. A., Oswalt T. D., 1998, ApJ, 497, 870
York D. et al., 2000, AJ, 120, 1579

This paper has been typeset from a TEX/LATEX file prepared by the author.